

The GETA Sandals: A Footprint Location Tracking System

Shun-yuan Yeh, Chon-in Wu, Keng-hao Chang, Hao-hua Chu, Jane Yung-jen Hsu

Department of Computer Science and Information Engineering
Graduate Institute of Networking and Multimedia
National Taiwan University
#1 Roosevelt Road, Section 4, Taipei, Taiwan 106
{r93124, r92079, r93018, hchu, yjhsu}@csie.ntu.edu.tw

Abstract.

This paper presents the design, implementation, and evaluation of a footprint-based indoor location system on traditional Japanese GETA sandals. Our footprint location system can significantly reduce the amount of infrastructure required in the deployed environment. In its simplest form, a user simply has to put on the GETA sandals to track his/her locations without any setup or calibration efforts. This makes our footprint method easy for everywhere deployment. The footprint location system is based on the dead-reckoning method. It works by measuring and tracking the displacement vectors along a trail of footprints (each displacement vector is formed by drawing a line between each pair of footprints). The position of a user can be calculated by summing up the current and all previous displacement vectors. Additional benefits of the footprint based method are that it does not have problems found in existing indoor location systems, such as obstacles, multi-path effects, signal noises, signal interferences, and dead spots. However, the footprint based method has two problems (limitations): (1) accumulative error over distance traveled, and (2) stair climbing and jumping motions. To address the first issue, it is combined with a light RFID infrastructure to correct its positioning error over some long distance traveled. Furthermore, it incorporates an accelerometer-based method to work under stair climbing and jumping motions.

1 Introduction

Physical locations of people and objects have been one of the most widely used context information in context-aware applications. To enable such location-aware applications in the indoor environment, many indoor location systems have been proposed in the past decade, such as Active Badge [1], Active Bat [2], Cricket [3], smart floor [4], RADAR [5], and Ekahau [6]. However, we have seen very limited market success of these indoor location systems outside of academic and industrial research labs.

We believe that the main obstacle that prevents their widespread adoption is that they require certain level of *system infrastructural support* (including hardware, installation, calibration, maintenance, etc.) inside the deployed environments. For example, Active Badge [1], Active Bat [2], and Cricket location systems [3] require the installation of infrared/ultrasonic transmitters (or receivers) at fixed locations (e.g., ceilings or high walls) in the environments. In order to attain high location accuracy and good coverage, the system infrastructure requires large number of transmitters (or receivers) installed in the deployed environments. This is beyond the reach of ordinary people to afford, operate, and maintain the infrastructure. WiFi based location systems such as RADAR [5] and Ekahau [6] require an existing WiFi network in the deployed environment. For example, the Ekahau location system recommends a WiFi client to be able to receive signals from 3~4 WiFi access points in order to attain the specified location accuracy of 3 meters. This high density of access points is unlikely in our everyday home and small office environments. In addition, most WiFi based location systems require users' calibration efforts to construct a radio map by taking measurements of WiFi signal strength at various points in the environment. This forms another barrier for users. Furthermore, the instability caused by dynamic environmental factors can also reduce the positioning accuracy and stability in the WiFi location systems [7]. Smart floor [4] can track the location of a user by using pressure or presence sensors underneath the floor tiles to detect the user's gait. This infrastructure cost is expensive because it requires custom-made floor tiles and flooring reconstruction.

Significantly reducing the needed system infrastructure serves as our main motivation to design and prototype a new *footprint location system* on traditional Japanese GETA (pronounced "gue-ta") sandals. This footprint location system can compute a user's physical location solely by using sensors installed on the GETA sandals. To enable location tracking, a user simply has to wear the GETA sandals with no extra user setup & calibration effort. This system works by attaching location sensors, including two ultrasonic-infrared-combo receivers and one ultrasonic-infrared-combo transmitter, on the GETA sandals. The basic idea can be described by looking at a person walking from location A to location B on a beach. He/she will leave a trail of footprints. To track a person's physical location, the system continuously measures a *displacement vector* formed between two advancing footprints (advancing in the temporal sense). To track a user's current location relative to a starting point, the system simply sums up all previous *footprint displacement vectors* leading to his/her current footprint location. This idea is similar to the so-called (deduced) *dead-reckoning navigation* dated back to the medieval time when the sailor/navigator located himself/herself by measuring the course and distance sailed from a starting point. In our system, this dead reckoning idea is adapted in tracking human footprints. We believe that having a *wearable location tracker* is an important advantage in our footprint location system over infrastructure-based indoor location systems. Users simply need to wear our GETA-like shoes, and our location system can work anywhere they want to go.

In addition to the benefit of low infrastructure cost, the *footprint location system does not have problems commonly found in existing indoor location systems*. For example, existing wireless based solutions (e.g., using radio, ultrasonic, or infrared)

can experience poor position accuracy when encountering obstacles between transmitters and receivers, multi-path effects, signal noises, signal interferences, and dead spots. On the other hand, our footprint location system avoids almost all of these problems. The reason is that the location sensors (ultrasonic-infrared transmitters and receivers) in our footprint method only need to cover a small sensing range, which is the short distance between two sandals in a maximum length of a walking step (< 1.5 meters). Assume walking on a relatively smooth surface, the footprint location sensors are unlikely to encounter any obstacles or experience multi-path effects, signal noises, and signal interferences over this small sensing range. This is in contrast to existing wireless (radio, ultrasonic, or infrared) based location systems where the sensing range must be large enough to cover the distance between fixed location sensors in the environment and a mobile location sensor on a user. This short sensing range in our footprint method also brings two additional advantages: (1) location sensors can significantly reduce its power consumption due to short sensing range, and (2) location sensors (ultrasonic-infrared) have high accuracy under such short sensing range (e.g., 0.2 mm in static setting).

There is one important shortcoming in our footprint location system called the *error accumulation* problem. It is inevitable that a small amount of error is introduced each time we take measurements to calculate a displacement vector. Consider a user has walked n steps away from a starting point. His/her current location is calculated as a sum of these n displacement vectors. This means that the current location error is also the sum of all errors from these n previous displacement vectors. In other words, the error in the current footprint measurement will be a percentage of the total distance traveled. To address this error accumulation problem, we utilize a small number of passive RFID tags with known location coordinates in the environment. A small RFID reader is also placed under a GETA sandal to read these RFID tags. Similar to NaviGeta [13], when a user walks on top of a location-aware RFID tag, the known location coordinate of that RFID tag is used instead of the calculated footprint location. Encountering a RFID tag has the same effect as resetting the accumulated error to zero. Although these location-aware RFID tags are considered system infrastructure, they constitute very light infrastructure because (1) RFID tags are relatively inexpensive in cost ($< \$1$ each) and easy to install, and (2) only a very small number of RFID tags are needed. Based on our measurements in Section 4, the average error per footstep is only about 4.6 mm . If we want to limit the average error to 46 cm , we only need to install enough RFID tags in the environment such that a user is likely to walk over a RFID tag approximately every 100 steps.

Although the signal obstacle problem seldom happens under normal walking environments, they can occur under the stair climbing where the stairs become the obstacles blocking ultrasonic signals transmitted between two sandals. This is the main limitation for the footprint location system [14]. Under this situation, the footprint-based system can not measure the displacement vector using ultrasonic devices between two advancing footprints. To address this limitation, the footprint-based system is combined with the accelerometer-based approach that computes footstep vectors using the sandal's acceleration data. Although the accelerometer-based method has lower accuracy than the ultrasonic footprint-based method, it is a good complement (or backup) method to improve the overall robustness of the system.

There are several pervious systems that are also based on incremental motion and dead reckoning. Lee et al [11] proposed a method to estimate the user’s current location by recognizing a sequence of incremental motions (e.g., 2 steps north followed by 40 steps east, etc.) from wearable sensors such as accelerometers, digital compass, etc. Lee’s proposed method differs from our footprint tracking system in that it can only recognize a few selected locations (e.g., bathroom, toilet, etc.) rather than track location coordinates. Point research [12] provides a vehicle self-tracking system that provides high location accuracy by combining the dead-reckoning method (wheel motions) and GPS. The solution from Point research differs from our method which is based on footprint tracking in normal human walking motion rather than mechanical wheel movements.

At the time of this paper writing, we have gone through four design-and-evaluation iterations. Rather than presenting only the final design and evaluation, we think that readers may also be interested to know these intermediate designs as well as mistakes we made on them. The remainder of this paper is organized as follows. Sections 2 to 5 describe our four design-and-evaluation iterations, including performance evaluations and discussions about design mistakes. Section 6 draws our summary and future work.

2 Initial design: Design Version I

The human walking motion can be modeled by stance-phase kinematics shown in Fig. 1. A forwarding walking motion is consisted of a sequence of three stances – *heel-strike*, *mid-stance*, and *toe-off*. In the heel-strike stance, the body weight pushes down from the upper body to the lower body, resulting in both feet in firm contact with the ground. This generates a footprint on the ground. In the mid-stance, the body raises one (left) foot forward and above the ground. In the toe-off stance, the body weight again pushes down on the forwarded (left) foot, again resulting in both feet in contact with the ground. This creates another footprint on the ground.

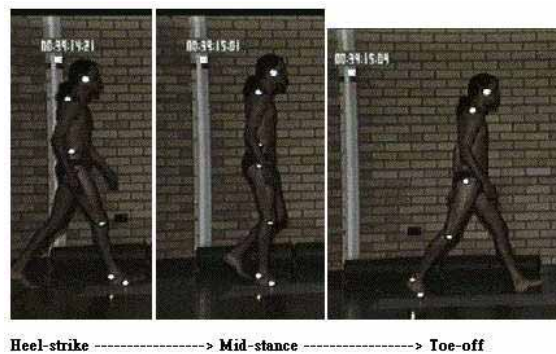


Fig. 1. Three stances in a normal human walking motion

The basic idea behind our footprint location tracking system is to (1) detect heel-strike and toe-off stances, and then (2) take measurement of two feet’s *displacement*

vector v_d (i.e., the footprint vector) on the ground. As shown in Fig. 2, given a starting point in a location tracking region (x_{start}, y_{start}) , e.g., the entrance of home or a building, we can compute the current position of a user, who has walked n number of steps away from the starting point, by summing up all displacement vectors $\sum_{i=1}^n v_{di}$, for $i=1..n$, corresponding to these n footsteps.

2.1 Footprint Positioning Algorithm

To measure the displacement vector v_d for each footprint, we place two ultrasonic-infrared-combo receivers on the left sandal and two ultrasonic-infrared-combo transmitters on right sandal shown in Fig. 3. The components for ultrasonic-infrared transmitters and receivers are obtained by disassembling the NAVInote's [8] electronic pen and base unit. In order to make both the receivers and transmitters face directly toward each other during normal walking motion¹, they are placed on the inner sides of the sandals. The prototype of the GETA sandals is shown in Fig. 7. Through NAVInote APIs, we obtain the (x, y) coordinates of these two transmitters located on the right sandal. Denote them as (x_{t1}, y_{t1}) and (x_{t2}, y_{t2}) as shown in Fig. 3. Note that the ultrasonic-infrared-combo technology can achieve very fine position accuracy and resolution at the short sensing range between two sandals. Under static setting, the measured average positioning error is $< 0.2mm$ and the resolution is $< 0.2mm$.

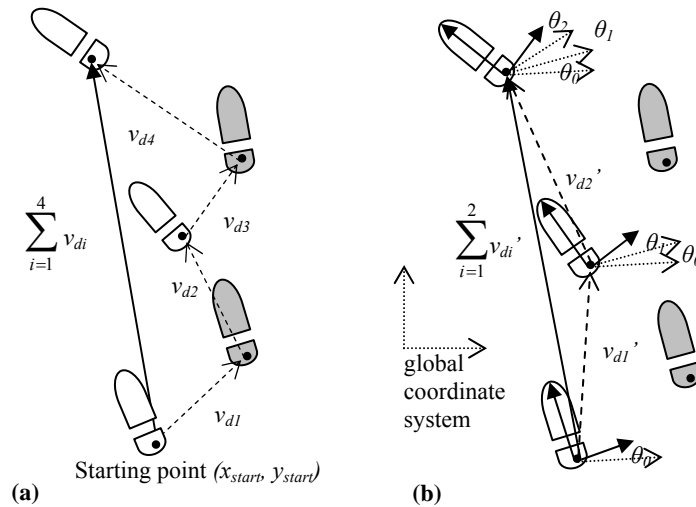


Fig. 2. The user has walked four footsteps 1-4. Fig. 2(a) shows these displacement vectors (v_{di}) corresponding to these displacement vectors. Fig. 2(b) shows θ_i as the rotational angel between the current local coordinate system and the previous local coordinate system in the previous footstep.

¹ We assume that people don't intentionally walk cross-legged.

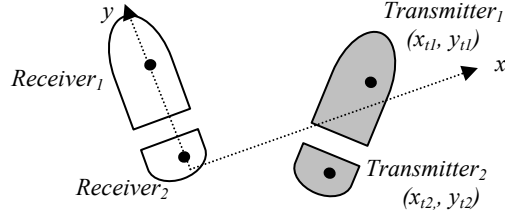


Fig. 3. It shows the locations of ultrasonic-infrared receivers and transmitters on the sandals. The coordinates of the transmitters on the right sandal is relative to the local coordinate system on the left sandal.

The coordinates of these two transmitters are measured relative to the *local coordinate system* of the left sandal, where the origin of this local coordinate system is at the heel position and the *y-axis* forms a straight line from the heel to the toes. Since moving left foot also changes the local coordinate system, it is necessary to *re-orientate* the displacement vector from its local coordinate system to a global coordinate system. The global coordinate system is set to be the coordinate of the starting point. To perform this orientation translation, we need to compute the *orientation angle* θ of the local coordinate system relative to the global coordinate system.

Denote the current step as the i -th left footstep. The orientation angle θ can be calculated as $\Sigma \theta_i$, where θ_i is the rotational angle between the i -th left footstep's coordinate system and the $(i-1)$ -th left footstep's coordinate system. This means that to compute the orientation angle θ , we need to compute θ_i for each new left footstep as illustrated in Fig. 2(b).

Fig. 4 shows (x_{i1}, y_{i1}) and (x_{i2}, y_{i2}) as the recorded coordinates of two transmitters on the right foot before moving the left foot, and (x_{i1}', y_{i1}') and (x_{i2}', y_{i2}') as their recorded coordinates after moving the left foot. As the left foot moves, the coordinate system on the left foot rotates θ_i and then translates into (dx, dy) . This gives us the following four sets of equations, which are sufficient to solve for three unknowns: θ_i and (dx, dy) .

$$\begin{bmatrix} \cos \theta_i & \sin \theta_i \\ -\sin \theta_i & \cos \theta_i \end{bmatrix} \begin{bmatrix} x_{i1} \\ y_{i1} \end{bmatrix} - \begin{bmatrix} dx \\ dy \end{bmatrix} = \begin{bmatrix} x_{i1}' \\ y_{i1}' \end{bmatrix}$$

$$\begin{bmatrix} \cos \theta_i & \sin \theta_i \\ -\sin \theta_i & \cos \theta_i \end{bmatrix} \begin{bmatrix} x_{i2} \\ y_{i2} \end{bmatrix} - \begin{bmatrix} dx \\ dy \end{bmatrix} = \begin{bmatrix} x_{i2}' \\ y_{i2}' \end{bmatrix}$$

We can then compute v_d using summed θ , dx , and dy .

$$\begin{bmatrix} \cos \theta & \sin \theta \\ -\sin \theta & \cos \theta \end{bmatrix} \begin{bmatrix} dx \\ dy \end{bmatrix} = v_d$$

Some readers might wonder why we use two transmitters instead of one transmitter. The reason is that one transmitter only gives two equations, which are insufficient

to solve three unknowns. With the additional transmitter, it can give two additional equations needed to solve three unknowns.

Prior to the above-mentioned geometry calculation, we need to detect the heel-strike and toe-off stances to measure (x_{i1}, y_{i1}) and (x_{i2}, y_{i2}) . We call these two stances the *steady state* because when both feet are in contact with the ground, the measured coordinates on two transmitters are *stable* (do not change much) for some small period of time. When we detect the steady state, we record the coordinates of two transmitters and then calculate the displacement vector.

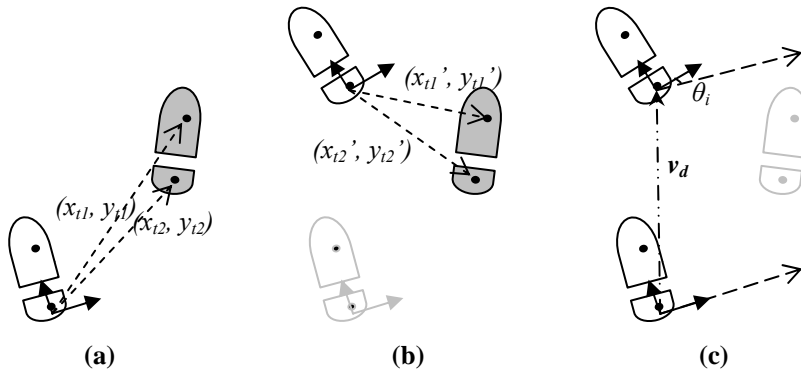


Fig. 4. Before moving the left foot, the coordinates of the transmitters on the right sandal, (x_{i1}, y_{i1}) and (x_{i2}, y_{i2}) , are recorded as shown in (a). After walking the left foot, (x_{i1}', y_{i1}') and (x_{i2}', y_{i2}') are recorded as shown in (b). To calculate v_d , we have to consider the rotation angel θ_i , translate (dx, dy) to the coordinate system of the left foot, and then transform them into the global coordinate system to get the displacement vector v_d as shown in (c).

Assume that the user moves the right foot and the left foot in an interleaving manner. We can track the position of the left foot by first computing two displacement vectors from left footprint to the right footprint and right footprint back to the left footprint.

2.2 Performance Evaluation

We have evaluated the performance of our initial design. The results have shown poor positioning accuracy. The main cause of poor accuracy is due to the interference of the signals from the two transmitters. Since the receivers can not distinguish two distinct signals from two transmitters, it can calculate incorrect coordinates on two transmitters. This leads to miss-detection of the steady state and incorrect calculation on the displacement vectors. Although we tried to filter out these incorrect coordinates, our results still showed high 49% rate of steady state miss-detections. When a miss-detection occurs, dx , dy , θ , and displacement vector will also be calculated in-

correctly. This leads to rapid error accumulation. Note that even a small error in the rotation angle θ , which is used to re-orient the displacement vector, can significantly reduce the position accuracy.

An additional problem is that we have not found a working method to distinguish if a person is moving forward or backward and which (left or right) foot is moving. This problem can be explained as follows. Consider the 1st case that a person is moving forward: if the right foot is moving forward, the x-coordinates of both transmitters will increase; on the other hand, if the left foot is moving forward, the x-coordinates of both transmitters will decrease. Consider the 2nd case that a person is moving backward, the situation is reverse, i.e., the x-coordinate will decrease (increase) when right (left) foot is moving backward. Given increasing x-coordinates on transmitters, it can be either right foot moving forward or the left foot moving backward. As a result, it is impossible to distinguish if a person is moving forward/background & left/right (foot movement).

3 Revised design: Design Version II

Design II tries to fix the following three problems from design I: (1) interferences from two transmitters, (2) incorrect detections of heel-strike and toe-off stances, and (3) indetermination of forward/backward & left/right movements. Design II solves these problems by incorporating additional sensors into the GETA sandals. To accurately detect the heel-strike and toe-off stances, we have added two force sensors at the bottom of both sandals to sense when both feet are in contact with the ground. These force sensors are also used to distinguish the forward/backward & left/right movements. To eliminate interferences from two transmitters, we remove one transmitter from the right sandal and incorporated an orientation sensor by InterSense InterTrax2 [9] on the front of left sandal. Fig. 7 shows the GETA sandal prototype of the revised design (version II).

3.1 Revised Footprint Positioning Algorithm

Since the orientation sensor can provide θ value for the global coordinate system, it removes one unknown in our calculation. This leads to a simpler algorithm than in version I. By measuring (x_i, y_i) and θ at the time of the heel-strike and toe-off stances, the displacement vector in the current footstep can be calculated by performing a simple rotational transformation. The displacement vector to the starting point is the sum of all the displacement vectors corresponding to the all previous footsteps.

3.2 Performance Evaluation

Fig. 5 shows the measured positioning error over different traveling distances and walking speeds. It has shown that two problems in design I have been addressed. The positioning accuracy is very good at short walking distances: the average error after

walking $5m$ is only $0.36m$, or approximately 6.8% . It also shows that our new design can accurately detect the heel-strike & toe-off stands, and then take measurements to compute the displacement vector. It can be seen that the error increases only slightly with increasing walking speed. However, we can clearly observe the problem of *error accumulation* in our footprint-only method, as the positioning error increases *super-linearly* with increasing walking distance.

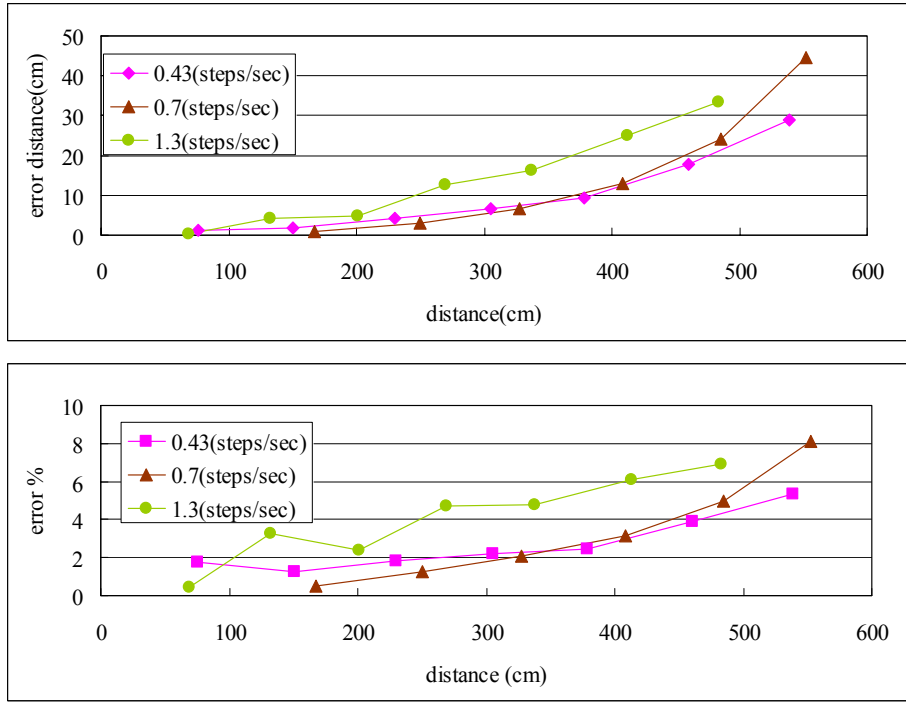


Fig. 5. The positioning accuracy (error) under different walking speeds over the walking distance.

The error is contributed from two main sources: (1) the displacement error vector from the ultrasonic-infrared-combo device, and (2) the orientation error from the orientation sensor. The displacement error is relatively small and stable due to the high accuracy in the ultrasonic-infrared-combo device. However, the displacement error is *accumulative* in future location calculation, so the error distance follows a linear growth pattern. Note that orientation error is more destructive than displacement error, i.e., even a one-time orientation error can make the positioning error grow linearly over walking distance. This can be explained by looking at Fig. 6. After the one-time orientation error of θ_{error} occurs, the calculated path will forever deviate from the real path, leading to linear growth in error displacement. In addition, we have found that our orientation sensor becomes inaccurate after rotating over 90 degrees. In order to get more accurate rotation angle θ , we reset the orientation sensor after

each left step, and then sum up each rotation θ_i to get the orientation θ . Due to this extra calculation, the orientation error of θ_i also becomes accumulative.

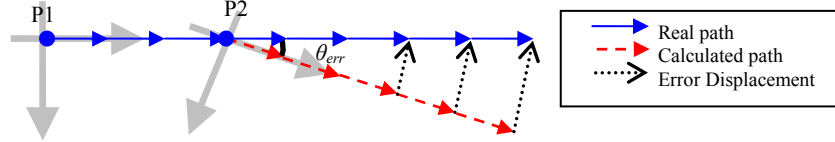


Fig. 6. Effect of error accumulation in θ

4 Revised design: Design Version III

Design III tries to fix the error accumulation problem in design II. Design III incorporates location-aware passive RFID tags & readers that can reset the accumulated error whenever the user steps on top of a RFID tag with a pre-determined location coordinate. These location-aware passive RFID tags forms a passive RFID grid that can be used to bound the accumulated error in design II. Since a higher RFID grid density means higher probability that a user will step on top of a passive RFID tag (therefore resetting the positioning error), the ideal density of the RFID grid can be chosen to achieve the needed positioning accuracy in the deployed environment.

The RFID solution has two parts: (1) a Skyetek M1[10] RFID reader is installed at the bottom of the left sandal, and (2) a set of passive RFID tags with the read range of 4.5 cm are placed in the grid fashion. We only attach one additional RFID reader to the left sandal, and the other device configuration is the same as in design II (Fig. 7.).

In the target environment, a server is used to maintain the table mappings between RFID tag IDs and corresponding location coordinates. When a user enters the target environment, the GETA sandal downloads its mapping table. The positioning algorithm is revised as follows. When the GETA sandal steps on top of a RFID tag, it looks up the cached mapping table to find the location coordinate of this RFID tag. Then, the current location of the user is set to the location coordinate of this RFID tag rather than from the footprint tracking method.

4.1 Performance Evaluation

We have evaluated the performance of GETA sandal (version III) in a 15×15 square meters testing environment. We have two different configurations of passive RFID grids. The first configuration places one tag every $3m$, and the second configuration places one tag every $5m$. Fig. 8 shows the measured positioning error over walking distance for these two configurations. The error is reset to zero when a user steps on top of a RFID tag. Fig. 8 also shows that under a random walk, there is a probability that a user may not step on a RFID tag every $3m$ or $5m$. As a result, the errors continue to accumulate past $3m$ or $5m$ until a user eventually steps over a RFID tag.

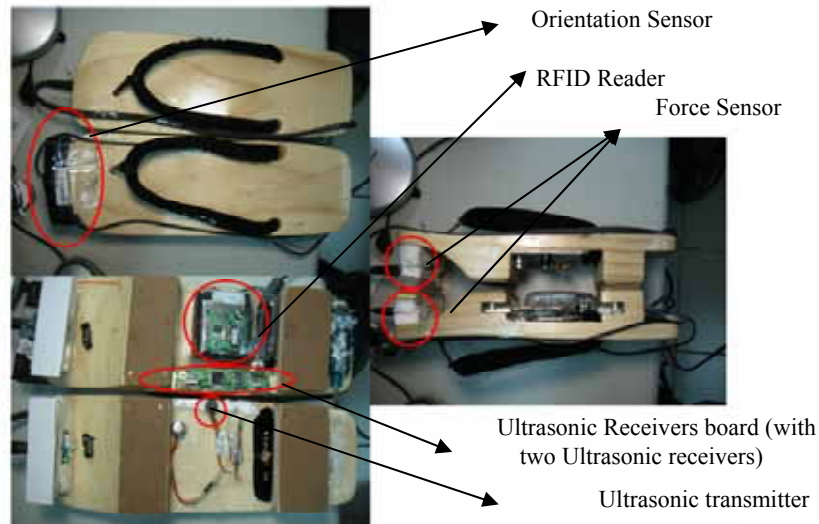


Fig. 7. It shows the prototype of final design (version III) of the GETA sandals. Prototype of design (version II) does not have the RFID reader. Prototype of design (version I) does not have the orientation sensor but has an additional transmitter.

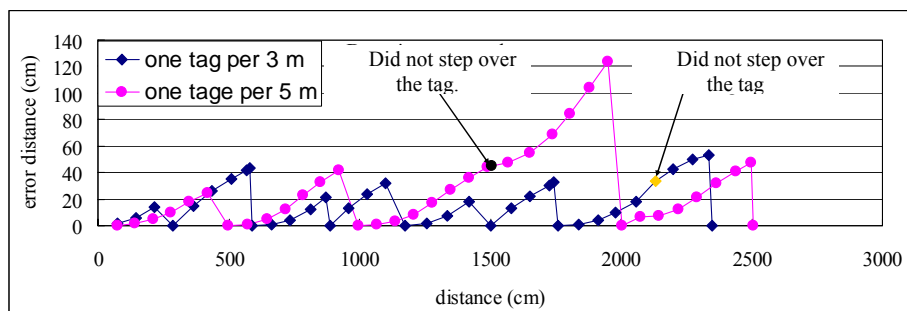


Fig. 8. The positioning accuracy (error) under different walking speeds over the walking distance.

5. Design Version IV

In the previous design versions, the footprint based method is based on measuring the distances between the ultrasonic/IR transmitters and receivers underneath the sandals. This approach has two basic limitations. The 1st limitation is when obstacles are between the two sandals, blocking signals from Ultrasonic/IR transmitters to receivers. For example, during stair climbing, the stairs become the obstacles blocking signals between two sandals. The 2nd limitation occurs when both feet move simultaneously.

For example, during a jumping motion, both feet are lifted off the ground and then touched down on the ground at approximately the same time. In other words, there are no heel-strike and toe-off stances to take measurement on the displacement vectors.

To address these two limitations, we have come up with design IV. It incorporates an *accelerometer* underneath one of the sandals to estimate the footstep vector. In a brief description (more details later), the *accelerometer-based method* consists of the following three main steps: (1) periodically sample the accelerometer readings, (2) apply double integral over the acceleration data to compute distance, and (3) combine the orientation sensor data to calculate the direction of traveled distance and to form the *step displacement vector*. The advantage of the accelerometer-based method over the ultrasonic footprint-based method is that it has no between-feet obstacle problem and works under jumping motions. However, its main drawback is lower positioning accuracy than the footprint-based method.

Since each has its perspective advantage and disadvantage, the accelerometer-based method is a good complement to the ultrasonic footprint-based method. Although the footprint-based method can achieve better positioning accuracy, it is also more prone to failures, e.g., under obstacle blocking and jumping motions, than the accelerometer-based method. On the other hand, although the accelerometer-based method has lower positioning accuracy, it does not have the obstacle blocking problem and works under jumping motion; hence it is more robust than the footprint-based method. By combining these two methods, it is possible to get *both better accuracy and robustness*. The combined method works as follows. At runtime, both methods are executed concurrently. If the footprint-based method can detect heel-strike and toe-off stances, we use the more accurate step vector from the footprint-based method. If not, the less accurate step vector from the accelerometer-based method is used.

In the following subsections, we will describe the accelerometer-based method in more details as well as its experimental evaluation.

5.1 Accelerometer-based Method

For the hardware components, a dual-axes accelerometer and a 3 dimension orientation sensor are installed underneath the left sandal. In addition, a force sensor is used to detect whether the left sandal is on or off the ground. Fig. 9 shows how the accelerometer-based method works. It is consisted of the following three steps: (1) the force sensor is used to detect when the left sandal is off the ground, indicating that the left sandal starts to move; (2) once the left sandal starts moving, synchronized streams of acceleration and the orientation data, from the accelerometer and orientation sensors, are collected at a rate of 50Hz until the force sensor detected that the left sandal is on the ground again, i.e. the left sandal has completed a step; and (3) the step displacement vector can be calculated by applying double integral over the synchronized streams of acceleration and orientation data. Since the first two steps are relatively straight-forward, no further explanation is needed. However, the third step involves

some complex issues. To address them, we describe two techniques called *acceleration compensation* and *double integral approximation*, as follows.

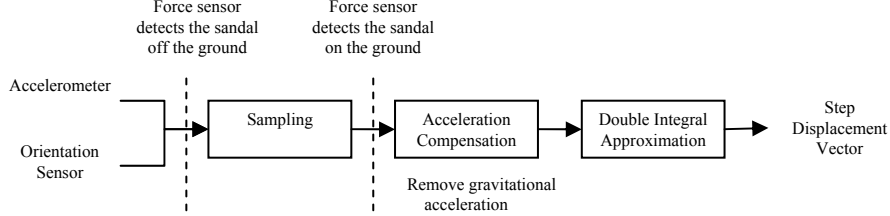


Fig. 9. Procedure of calculating step displacement vector in the accelerometer-based method

Acceleration Compensation

The task for the acceleration compensation is to *filter out* the effect of gravitational acceleration from the acceleration readings and leave only the clean acceleration produced by the moving motion. This *clean* acceleration readings can then be used by the double integral algorithm to estimate distances in the step displacement vectors. To see why this filtering process is needed, consider the example in Fig. 10. The dual-axes accelerometer is placed flatly on the horizontal surface underneath the sandals to measure acceleration on the x and y axes. During a normal walking motion, the sandal is likely to be tilted horizontally from time to time, i.e., being not perfectly parallel to the earth's horizontal plane. Using air navigation terms, tilting over the y axis is called a *pitch* with a pitch angle (θ_{Pitch}), and tilting over the x axis is called a *roll* with a rolling angle (θ_{Roll}). The problem with a roll or a pitch is when the axis of the sandal forms an angle with the horizontal plane, the accelerometer will register gravitational force readings on the x and y axes, even if the sandal has not moved but only tilted. In other words, the raw accelerometer reading reflects a combination of the gravitational acceleration produced by sandal's horizontal tilting and its moving acceleration. To calculate the correct step displacement vector, the gravitational acceleration needs to be filtered out from the accelerometer readings.

To address this issue, a 3D orientation sensor is used to measure both the pitch and the rolling angles. We can then compensate the acceleration using the following formulas:

$$\begin{aligned}
 a'_x &= (a_x + g * \sin(\theta_{Pitch})) \cos(\theta_{Pitch}) \\
 a'_y &= (a_y - g * \sin(\theta_{Roll})) \cos(\theta_{Roll})
 \end{aligned}$$

The variables a_x and a_y are the raw acceleration readings in the x and y axes from the accelerometer. a'_x and a'_y are the *filtered* acceleration readings, free from gravitational acceleration, in the x and y axes. g is the gravitational acceleration. The term ($g * \sin(\theta)$) represents the portion of gravitational acceleration produced from a pitch or roll. The term $\cos(\theta)$ is used to project the amount of acceleration to the horizontal plane.

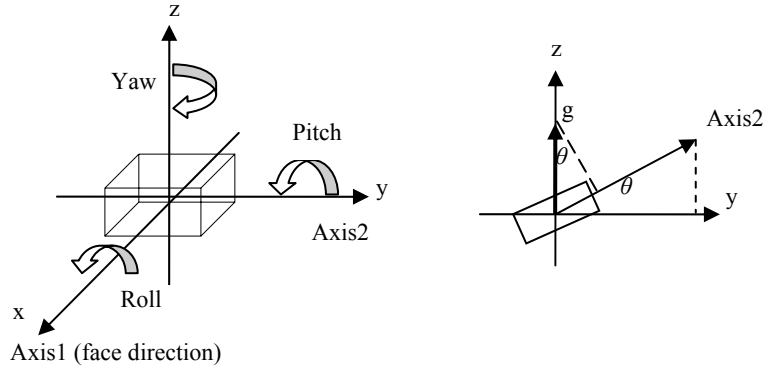


Fig. 10. Acceleration Compensation. A dual-axis accelerometer is placed flatly on axis-1/axis-2, parallel to the horizontal plane (x - y plane). It measures accelerations in both directions. When the sandal is off the ground, sandal tilting causes the accelerometer to rotate in a roll and a pitch direction, creating an angle θ_{Pitch} on the axis-1 and an angle θ_{Roll} on the axis-2 to the horizontal plane. For example, sandal tilting creates an angle θ_{Roll} between the axis-2 and the y -axis shown on the right drawing. Therefore, acceleration compensation needs to remove the gravitational acceleration $g * \sin(\theta_{Roll})$ from the raw acceleration reading.

Double Integral Approximation

Since the accelerometer readings are discrete-time signals, they can be modeled as discrete-time points on a nonlinear curve corresponding to the movement path of a forward moving footstep shown in Fig. 11. Each discrete-time point contains the following information $(a'_x, a'_y, \theta_{Yaw})$, where (a'_x, a'_y) are the filtered acceleration of the sandal in the x and y directions, and θ_{Yaw} is the direction of the acceleration on the horizontal plane obtained from the orientation sensor. A *full step displacement vector* (shown as the red line in Fig. 11) can be calculated as the sum of these multiple *piece-wise vectors* (shown as blue lines in Fig. 11), which are in turn computed by applying double-integral using the trapezoidal rule on these discrete-time acceleration data. However, there is a problem in the different orientations of the coordinate systems where these piece-wise vectors are derived. For example, Fig. 11 shows that the coordinate system in the 2nd piece-wise step vector is slightly rotated in the clockwise direction from the coordinate system in the 1st piece-wise step. Given different coordination systems, we cannot simply sum these piece-wise vectors to obtain the full step displacement vector. This problem is similar the coordinate system transformation in the footprint based method described in Section 2.

To address this problem, these piece-wise displacement vectors are transformed to a *global coordinate system*, which is the coordinate system of the first point, before summing them up to calculate the full step vector.

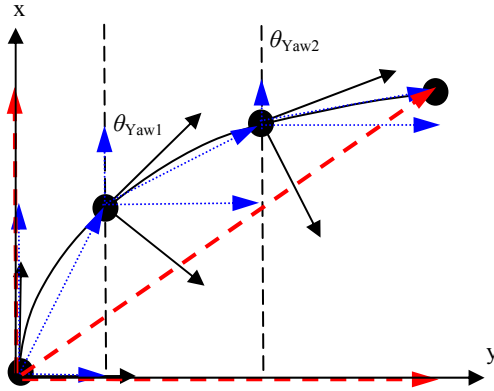


Fig. 11. Double Integral Approximation. The black-colored curve is a trace of a turning right motion. The black-colored points are the sampled acceleration points. The black solid arrows represent the directions of the sampled acceleration. At each sampling point, we read two acceleration data in the x-y directions, the acceleration direction on the x-y plane, and the angle *Yaw* denoting the amount of the angle rotation to the global coordinate system.

5.2 Performance Evaluation

We have performed the following experiments to evaluate the positioning accuracy in the accelerometer-based method: the one-step experiment, the straight-line experiment, and the stair-climbing experiment.

One-step Experiment

The one-step experiment involves a user, standing at an origin point, moves a single step to eight different directions shown in Fig. 12. In each direction, we conducted 15~25 different trials. The results are plotted in Fig. 12. The actual positions of the sandal are marked as red square points. The estimated locations using the accelerometer-based method are marked as smaller pink dots. The mean estimated locations are marked as blue diamond points. Fig. 12 shows that the positions for left and back steps are over-estimated (overshooting the real positions), whereas the positions for the right and forward steps are under-estimated (falling short of the real positions). The mean error is 9 *cm* with the standard deviation of 3.6 *cm* over a 44 *cm* mean step size.

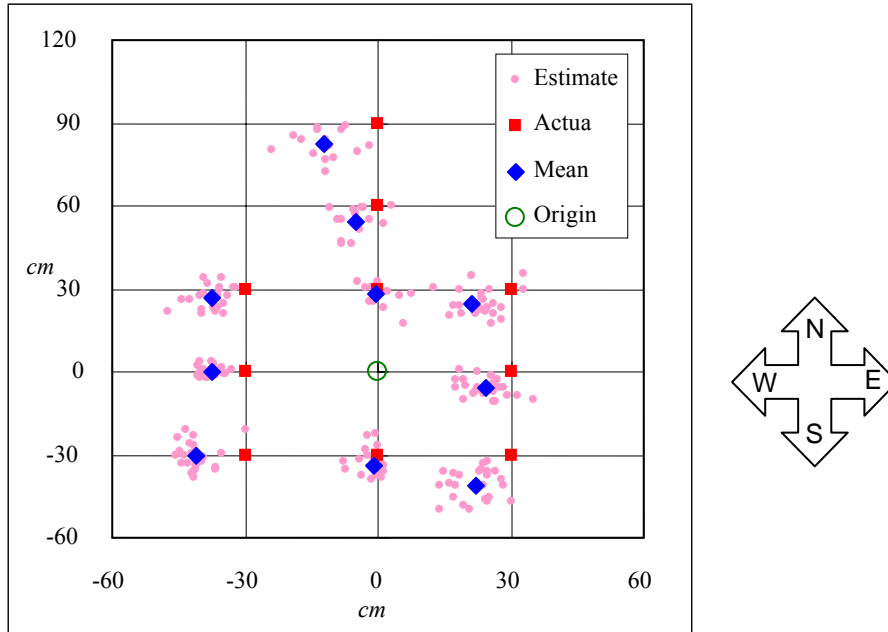


Fig. 12. Estimated positions vs. the actual positions in the one-step experiment.

Table 1. It shows the mean error and the standard deviation in each directional step.

	N30	N60	N90	S	E	W	NE	NW	SE	SW
Mean Error (cm)	3.6	8.6	15.1	5.6	9.3	7.8	11.7	9.1	14.3	12.0
Mean Error (%)	12	14.3	16.8	18.7	31	26	27.6	21.5	33.7	28.2
Standard Deviation	1.8	4.2	5.2	2.1	2.9	2.4	6.1	4.1	5.2	2.7

Straight-line Walking Experiment

The *straight-line walking* experiment involves a user walking a straight line of length 12 meters. Fig. 13 shows the positioning error over the distance traveled over three repeating traces. The walking speed is approximately 0.4 ~ 1.0 m/sec. The mean positioning error is approximately 13.2% or 1.58 meters, over 12 meters traveled.

Fig.13 shows that the accelerometer-based method achieves lower positioning accuracy than the footprint-based method. The positioning error of the footprint-based method in the design III is approximately 5.4% or 0.29 meters (over 5 meters traveled), while the positioning error of the accelerometer-based method is 9% or 0.5 meters.

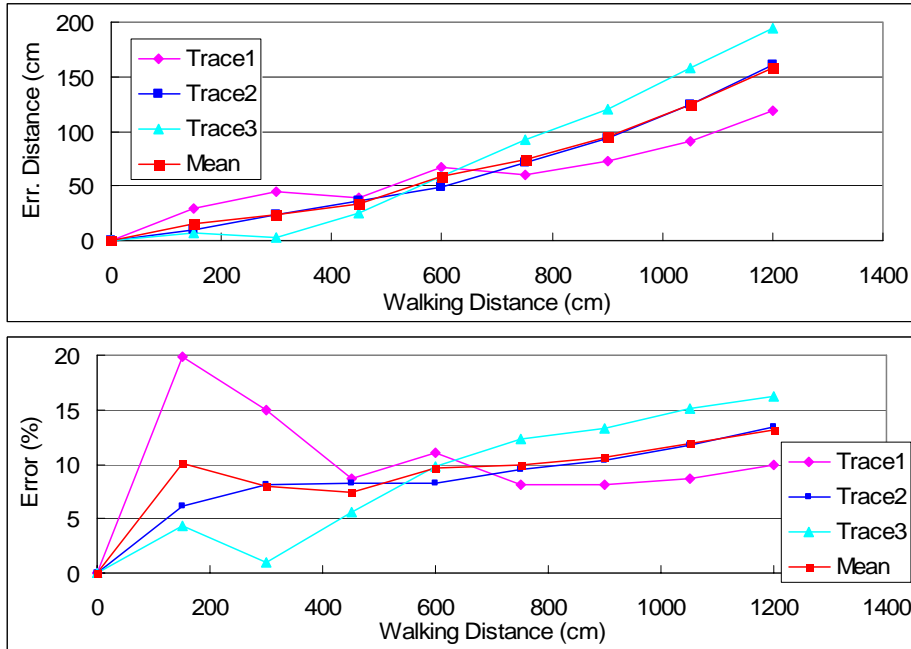


Fig. 13. Positioning error vs. walking distance in the straight-line walking experiment.

Stair Climbing Experiment

The stair climbing experiment involves a user climbing one floor of stairs in our department building shown in Fig. 14. The total number of climbed steps is 22. In the experiment, each trace start at one location (0,0) on a lower floor and end at the same location (0,0) on a upper floor. The estimated traces in Fig. 14 started on the 2nd, 3rd, and 4th floor respectively. The total traced distance is 10.4 meters. The horizontal walking speed is about 0.35 *m/sec*. The accumulative positioning errors of the three traces measured at the end of stair climbing are 0.21 *m* (2%), 0.67 *m* (6.4%), and 1.23 *m* (11%) respectively. The mean positioning error is 6.8% (0.70 *m*) over 10.4 meters traveled. Fig. 15 shows the accumulated error versus the climbed distance.

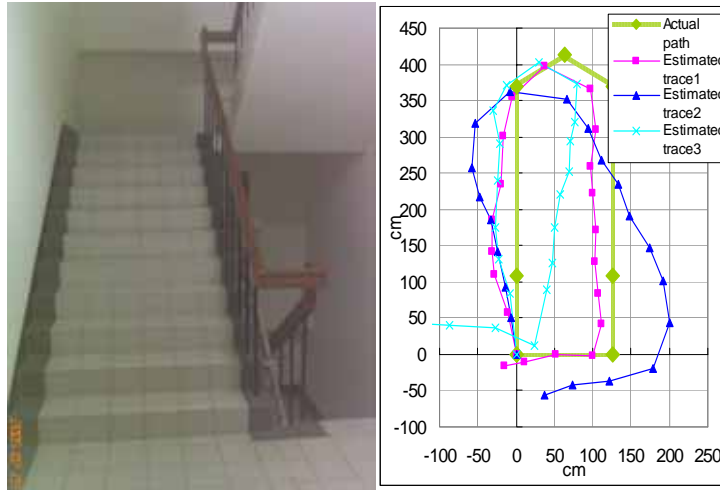


Fig. 14. The left picture shows the stair climbing environment. The right graph plots the three estimated traces in the stair climbing.

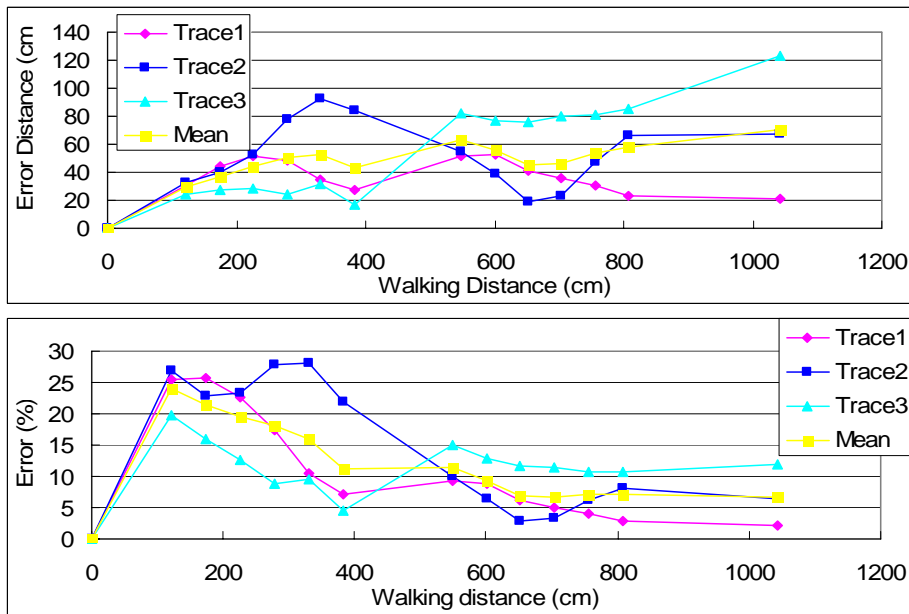


Fig. 15. Positioning error vs. climbed distance in the stair climbing experiment.

6. Conclusion and Future Work

This paper describes the design, implementation, and evaluation of our footprint-based and accelerometer-based indoor location systems on traditional Japanese GETA sandals. These systems can significantly reduce the amount of infrastructure needed in the deployed indoor environments. In its simplest form, these systems are contained within the mobile GETA sandals, making it easy for everywhere deployment. The user simply has to wear the GETA sandals to enable his/her location tracking with no efforts in calibration and setup. In addition to the benefit of being low infrastructure cost, the footprint based method has fewer problems in infrastructure-based indoor location systems such as noises, obstacles, interferences, and dead spots. Although the footprint based method can achieve high accuracy per moving footstep, we have encountered several problems that have been addressed in this paper. (1) Since the positioning error can be accumulated over distance traveled, it may need to be combined with a light RFID infrastructure to correct its positioning error over some long distance traveled. (2) Since the footprint-based method has limitations in situations such as stair climbing and jumping motions, it is combined with the accelerometer-based approach to improve the robustness of the system.

There are two yet-to-be-addressed problems in our current prototype of GETA sandals: wear-ability and RFID tag placement. The current wear-ability is unsatisfactory due to interconnecting all sensor components to a Notebook PC through hardwiring. In our next prototype, we would like to replace all hardwiring with wireless networking (e.g., Bluetooth), and replace processing on the Notebook with a small embedded processor. To further reduce the RFID infrastructure, we are interested to locate strategic frequently visited spots in an environment and to place these RFID tags.

References

1. R. Want, A. Hopper, V. Falcao, and J. Gibbons. The Active Badge Location System. *ACM Transaction on Information Systems*, 10:1, pp. 91-102, 1992.
2. A. Harter, A. Hopper, P. Steggle, A. Ward, and P. Webster. The anatomy of a context-aware application. In *Proc. of 5th MOBICOM*, pages 59–68, 1999.
3. N. B. Priyantha, A. Chakraborty, and H. Balakrishnan. The Cricket Location-Support System. In *Proc. of the 6th MOBICOM*, Boston, MA, USA, August 2000.
4. R. J. Orr and G. D. Abowd. The Smart Floor: A Mechanism for Natural User Identification and Tracking. *GVU Technical Report GIT-GVU-00-02*, 2000.
5. P. Bahl and V. Padmanabhan. RADAR: An In-Building RF-based User Location and Tracking System. In *Proc. of the IEEE INFOCOM 2000*, pages 775-784, March 2000.
6. Ekahau, <http://www.ekahau.com/>
7. Yi-Chao Chen, Ji-Rung. Chiang, Hao-hua Chu, Polly Huang, and Arvin Wen Tsui, Sensor-Assisted Wi-Fi Indoor Location System for Adapting to Environ-

- mental Dynamics, in ACM/IEEE International Symposium on Modeling, Analysis and Simulation of Wireless and Mobile Systems (*MSWIM 2005*), Montreal, Quebec, October 2005.
8. NaviNote technology, <http://www.navinote.com>
 9. InterSense, <http://www.isense.com>
 10. Skyetek RFID engineering, <http://www.skyetek.com/index.php>
 11. E. Foxlin and L. Naimark. Miniaturization, Calibration, Accuracy Evaluation of a Hybrid Self-Tracker, IEEE/ACM International Symposium on Mixed and Augmented Reality (ISMAR 2003), Oct. 2003.
 12. Point Research Corp., <http://www.pointresearch.com/>
 13. S. Itiro, <http://sio.jp/projects/idcarpet/index.html>
 14. Kenji Okuda, Shun-yuan Yeh, Chon-in Wu, Keng-hao Chang, Hao-hua Chu, The GETA Sandals: A Footprint Location Tracking System, Workshop on Location- and Context-Awareness (*LoCa 2005*), in Cooperation with Pervasive 2005, (also published as Lecture Notes in Computer Science 3479, Location- and Context-Awareness), Munich, Germany, May 2005, pages 120-131.